Nonconservation of parity in the elastic neutron-nucleus interaction channel

V. P. Alfimenkov

Joint Institute for Nuclear Research, Dubna

Usp. Fiz. Nauk **144**, 361–380 (November 1984)

The history of studies of nonconservation of parity in the elastic neutron-nucleus interaction channel is discussed. A brief account is given of the theory of the phenomenon, and experimental work in this field is reviewed. Experimental data are discussed and compared with theoretical predictions.

CONTENTS

1. INTRODUCTION

Following the discovery of nonconservation of parity in weak interactions, Feynman and Gell-Mann in 1957 put forward the hypothesis of universal weak interaction between fermions. A possible way of verifying this hypothesis was to detect the nonconservation of spatial parity in nucleon-nucleon interactions and then to compare the scale of observed nonconservation with that predicted on the basis of this hypothesis. The hypothesis suggests that the nucleon-nucleon potential should have the form

$$v = v_0 + w, \tag{1}$$

where v_0 conserves parity and w does not. Model-based estimates of the relative strength of the two components of the interaction gave

$$F_0 = \left(\frac{w}{v_0}\right)_{\text{eff}} = 10^{-7} - 10^{-6}. \tag{2}$$

Interference processes that are linear in the interaction and are due to the mixing of states with different parities should be of the same order.

The advent of the hypothesis of universal weak interaction was immediately followed by discussions of possible experimental verification of the nonconservation of parity in nuclear processes. To a considerable extent, this was due to the advanced state of technology and methodology that were by then available in nuclear physics for the investigation of fine effects.

The universal weak interaction hypothesis enables us to write the Hamiltonian for the interaction between nucleons in the nucleus in the form

$$H = H_0 + W, \tag{3}$$

where W is a small term representing parity-nonconservation in weak interactions. In the simplest single-particle nuclear processes, for example, in potential scattering of nucleons by nuclei, the expected parity nonconservation effects are of the order of F_0. In complex nuclear processes, such effects can be both suppressed and enhanced. It was therefore natural to look for situations in which parity nonconservation would be enhanced in nuclear interactions. An important step in this search was made in 1959–1960 by de Haas *et al.*, I. S. Shapiro, and Blin-Stoyle, who pointed out that the mixing of excited states of different parity and the same spin in complex nuclei could be considerably enhanced when these states had similar energies. This enhancement of the mixing of levels is now referred to as dynamic enhancement.

The presence in the Hamiltonian (3) of a parity-violating term W can lead to the appearance of small terms that are odd under space inversion and can be observed experimentally. Accordingly, quantities that are usually examined experimentally (such as cross sections, angular distributions, and so on) can be written in the form

$$S = S_0 (1 + F), \tag{4}$$

where F is a pseudoscalar, i.e., a *P*-odd quantity. For microparticles, the simplest such quantity, or, as is often said, a *P*-odd correlation, is the scalar product of momentum $\mathbf{p}$ and spin $\mathbf{s}$. A possible expression for F is, therefore,

$$F = \mathcal{F}_0 \frac{\mathbf{p}\cdot\mathbf{s}}{ps}, \tag{5}$$

where $\mathcal{F}_0$ is a constant characterizing the given process. The efforts of experimenters have, in fact, been directed toward searches for relationships of the form

$$S = S_0 \left(1 + \mathcal{F}_0 \frac{\mathbf{p}\cdot\mathbf{s}}{ps}\right) \tag{6}$$

whenever *P*-odd effects were expected to be appreciable.

These efforts were first crowned with success in 1964. The Abov group at the Institute of Theoretical and Experimental Physics showed[1] that the angular distribution of γ-rays emitted as a result of thermal-neutron capture by ^{113}Cd was slightly anisotropic relative to the spin direction of the captured neutrons, i.e., the corresponding angular distributions contained a term of the form

 0038-5670/84/110797-12$01.80

$$F = \mathcal{F}_0 \frac{\mathbf{p}_\gamma \mathbf{s}}{p_\gamma s}, \quad (7)$$

where $\mathbf{p}_\gamma$ is the momentum of the γ-ray and $\mathbf{s}$ the spin of the neutron. The P-odd correlation $\mathbf{p}_\gamma \mathbf{s}$ was confirmed experimentally. A related P-odd phenomenon was also found later. It was discovered[2] that γ-rays produced as a result of the radiative capture of unpolarized thermal neutrons by unpolarized nuclei had a small degree of circular polarization. Here, we are concerned with the P-odd correlation $\mathbf{p}_\gamma \mathbf{s}_\gamma$, where $\mathbf{s}_\gamma$ is the spin of the γ-quantum. The size of both these effects was of the order of 10^{-4}. It was thus shown that parity conservation violated in nuclear interactions, and that this violation was substantially greater than the single-particle estimate of $\mathcal{F}_0$. The considerable enhancement of P-odd nuclear effects was, on the one hand, a favorable circumstance because it facilitated reliable observation of these effects. On the other hand, modern nuclear theory was not in a state to provide reliable information about the magnitude of the corresponding enhancement coefficients. Experimental information on P-odd effects in nuclear interactions cannot, therefore, be used to obtain reliable quantitative information on parity-violating nucleon-nucleon interactions, i.e., a final confirmation of the hypothesis of universal weak interaction.

In 1977, Danilyan's group, again working at the Institute for Theoretical and Experimental Physics, observed a further P-odd effect in nuclear interactions. They found[3] an asymmetry in the angular distribution of the light (or heavy) fission fragment relative to the spin direction of the thermal neutron captured by the target nucleus. The corresponding fragment angular distribution had the form given by (4) with

$$F = \mathcal{F}_0 \frac{\mathbf{p}_f \mathbf{s}}{p_f s} \quad (8)$$

where $\mathbf{p}_f$ was the fragment momentum. The quantity $\mathcal{F}_0$ turned out to be of the same order as for the capture γ-rays. This result was so unexpected that, until it was confirmed by other workers, there were some doubts as to the whether the experiment was correctly performed. Such a large effect in fission was difficult to understand within the framework of the model used to explain the large enhancement of P-odd effects in radiative capture.[4] The difference between the two effects is that, in radiative capture, the effect is observed for γ-rays corresponding to transitions between two definite nuclear states, whereas, in fission, the effect is averaged over a large number of individual transitions corresponding to the formation of the so-called light fragment. It was believed at the time that effects associated with different transitions had random signs, which should have led to a strong suppression of the average effect observed in fission. In reality, this supression does not occur, i.e., the signs of the effects corresponding to different individual transitions are relatively rigidly correlated. The reason for this correlation must be sought in the properties of the fission process itself, and appear to be due to the "cold" stage of fission that immediately precedes the breaking of the "neck" between the two already formed fragments.

Possible experimental verifications of P-odd effects in the elastic channel of the neutron–nucleus interaction began to be discussed in the middle sixties. This class of effects includes not only neutron scatttering itself, but also effects that can be seen in the total neutron-nucleus interaction cross sections. The basis for this is the optical theorem of quantum mechanics which relates the total cross section to the elastic forward-scattering amplitude. For a long time (about 15 years), the discussion was confined to the single-particle interaction between neutrons and nuclei,[5–9] in which the nucleus was considered to be free of internal structure. The interaction was described by the Hamiltonian

$$H = H_0 + W \frac{\mathbf{p}_n \mathbf{s}}{p_n s}, \quad (9)$$

where $(W/H_0)_{\text{eff}} \simeq F_0$ and $\mathbf{p}_n$ and $\mathbf{s}$ are the momentum and spin of the neutron, respectively. The two cases $\mathbf{p}_n \mathbf{s}/p_n s$, i.e., those of neutrons with positive and negative helicity, should correspond to somewhat different scattering amplitude and total cross section. In complete analogy with ordinary optics, these differences should give rise to neutron-optical birefringence and dichroism. Birefringence produces rotation of the neutron polarization around the neutron momentum as the beam penetrates the medium. Dichroism, on the other hand, ensures that the transparency of the target is a function of neutron helicity. Estiamtes of the rotation of polarization (in radians) and the relative change in transparency for targets of thickness equal to one neutron mean free path led to values of the order of 10^{-6}–10^{-7}, which could not be measured. It was suggested[8] that the effects could be substantially enhanced by using neutrons with energies close to certain hypothetical single-particle resonances in complex nuclei.

It is now difficult to understand why the effect of the complicated structure of the nucleus on processes in the elastic channel was not included in this discussion. Indeed, it had been reliably established that it was precisely this complexity that led to very considerable enhancement of P-odd effects in the inelastic neutron-nucleus interaction channels. There were also theoretical publications[10] relating P-odd circular polarization of γ-rays from the radiative capture of neutrons, on the one hand, and p-resonances in nuclei, on the other. These interesting papers which, unfortunately, passed unnoticed, derived expressions for the effect, which indicated resonance behavior and enhancement due to the kinematics of the process.

In the middle of 1980, the ILL (Grenoble) group led by Forte published[11] an experimental paper in which P-odd neutron-optical birefringence and dichroism were confirmed for the interaction between polarized cold neutrons and unpolarized ^{117}Sn nuclei. They followed the "single-particle ideology" and looked for P-odd effects on the ^{124}Sn nucleus with a p-resonance at 62 eV, which was thought to be to a large extent of single-particle origin. The effect was not observed for ^{124}Sn but, unexpectedly for these workers, the effect was found to be present in a control specimen of natural tin. Subsequent studies showed that this was due to ^{117}Sn, on which the effect was enhanced by two or three orders of magnitude as compared with single-particle estimates, and so were the above P-odd effects in inelastic channels of the neutron-nucleus interaction.

The experimentally confirmed enhancement of P-odd

effects in the elastic neutron-nucleus interaction channel was explained in a theoretical paper by Sushkov and Flambaum,[12] which appeared almost simultaneously with the results of the Forte group. Sushkov and Flambaum finally took into account the influence of the complex structure of nuclei on P-odd effects in the elastic channel, using a model involving the mixing of nuclear compound states. In this model, the P-odd effects are due to the mixing of excited nuclear states of opposite parity and the same spin by a small P-odd correction W to the total nuclear Hamiltonian (3). The P-odd effects in complex nuclei turn out to be considerably enhanced by the dynamic enhancement of the mixing of compound levels and, under certain definite conditions, by the kinematics of the process. Sushkov and Flambaum also noted that these effects should be very dependent on neutron energy near the appropriate p-resonances of complex nuclei and, in favorable cases, may reach values of 0.01–0.1.

Since the middle of 1981, experimental papers by groups at the Leningrad Institute of Nuclear Physics[13,14] and the Neutron Physics Laboratory of the Joint Institute for Nuclear Research[15,18] reported studies of the dependence of total neutron cross sections on neutron helicity (P-odd neutron-optical dichroism). The Leningrad experiments utilized polarized thermal neturons and showed that the observed effects were due to the component of the total neutron cross section associated with the formation of the compound nucleus.

At NPL-JINR which, at the time, apparently had the only beam of polarized resonance neutrons in the world, the effect was investigated near weak p-resonances of certain nuclei. Some of the nuclei were found to exhibit a considerable enhancement of the effect at the p-resonances, and the dependence of this on neutron energy was observed.

The paper by Sushkov and Flambaum[12] was followed by a number of theoretical studies of this question.[20–27] Most of them employed the same model of mixing compound states. It was only in the recent paper by Zaretskiĭ and Sirotkin[27] that a different model was considered, namely, the mixing of single-particle components of compound-nucleus wave functions in the continuous spectrum (this mechanism is analogous to the valence mechanism in radiative neutron capture). The question as to which of these models provides a better description of reality is now being intensively discussed by theoreticians. The question could be resolved experimentally. However, the difference between the predictions of these two models involves very fine, and therefore difficult to observe, effects. Existing experimental information is clearly inadequate to enable us to choose between the two models.

In the account given below, we shall use the model of mixing compound states, which is older and more widely employed. Existing experimental data on the phenomena are satisfactorily explained by this model. It is important to note, however, that quantitative comparison between theoretical and experimental results is complicated by the inability of modern theory to calculate some of the quantities that appear in it, and by the absence of experimental data on a number of the parameters of mixing states that are essential for this comparison.

2. BASIC ASSUMPTIONS OF THE THEORY

P-odd neutron-optical dichroism and birefringence in which we are interested can be naturally related to the dependence of the elastic forward-scattering neutron amplitude of the neutron helicity. Let us examine this question. There are well-known relationships between the elastic forward-scattering neutron amplitude $f(0)$ and the total neutron cross section σ, on the one hand, and the refractive index n for neutron waves, on the other:

$$\sigma = \frac{4\pi}{k} \operatorname{Im} f(0), \tag{7'}$$

$$n = 1 + \frac{2\pi}{k^2} N \operatorname{Re} f(0); \tag{8'}$$

where k is the neutron wave number and N the number of nuclei per unit volume of the target. P-odd dichroism means that the cross sections σ_+ and σ_- for neutrons with opposite helicites are not equal. In its turn, the difference betweeen n_+ and n_- (birefringence) leads to the rotation of neutron polarization around the neutron momentum. The relation between n_+ and n_-, on the one hand, and this rotation, on the other, can be readily obtained as follows. The spin wave function describing the polarization of the beam is given by the well-known expression

$$\chi = c_+\chi_+ + c_-\chi_-, \tag{9'}$$

where $\chi_\pm$ are the neutron wave functions with the two possible spin components $s_z = \pm 1/2$ along the quantization axis, and $c_\pm = |c_\pm| e^{i\Phi_\pm}$ are the probability amplitudes for these states. For a beam polarized at right angles to the z axis, the angle between the x axis and the direction of polarization is related to $\Phi_\pm$ by

$$\varphi = \Phi_- - \Phi_+, \tag{10}$$

where the angle is measured clockwise from the positive direction of the x axis. To be specific, let us suppose that the neutrons move in the direction of the z axis. As the beam traverses a thickness z of the medium, the phases $\Phi_\pm$ are increased by $\Delta\Phi_\pm + kzn_\pm$, i.e., the polarization rotates around the z axis (neutron momentum) through the angle

$$\Delta\varphi = kz\,(n_- - n_+). \tag{11}$$

Thus, to describe the above phenomena, it is sufficient to obtain the elastic forward-scattering amplitude for neutrons with positive and negative helicity. As noted above, P-odd effects in processes involving the formation of the compound nucleus are much more pronounced than the analogous effects in single-particle processes. This means that we may exclude potential scattering from our analysis. Since the phenomena that we are discussing produce numerically small effects, we can use perturbation theory for processes proceeding through the compound nucleus.

We begin by considering the mixing of nuclear states with the same spin but opposite parity in relation to processes in the elastic channel for relatively complex nuclei and low-energy neutrons for which the effects under consideration can be detected experimentally. The excited states of nuclei can be examined by studying the so-called neutron resonances that appear when neutrons interact with nuclei. Resonances excited by neutrons with orbital angular momentum $l = 0, 1, 2, \ldots$ are called s-, p-, d-, ... resonances.

Even and odd l correspond to compound-nucleus states with opposite parities. For the slow neutrons that we are considering here, the neutron-nucleus cross section falls off rapidly with increasing l. We may therefore confine our attention to s- and p-resonances when we consider parity nonconservation effects in processes proceeding through the elastic channel. For nuclei with spin $I>0$, we need only consider p-resonances with spins $J=I\pm 1/2$ (for $I=0$, we have $J=1/2$) because the necessary condition for mixing is that the resonances must have equal spins. A given resonance, for example, the p-resonance, is mixed by the parity-violating interaction with all the s-resonances of the same spin, but it follows from simple perturbation theory, and will be demonstrated below, that the mixing rate falls off rapidly with increasing energy separation between the mixing resonances. This means that, when we consider P-odd effects, we can confine our attention to the so-called two-level approximation, i.e., we need only take into account the mixing of the two nearest resonances of opposite parity. Comparison of theoretical predictions with existing experimental data shows that the two-level approximation is good enough. However, in some cases, especially for nuclei with high density of resonances, the approximation may turn out to be unsatisfactory.

The expressions for the P-odd dependence of forward-scattering amplitude on neutron helicity is most readily obtained by the diagram method. This instructive perturbation-theory technique was put forward by Feynman in the 1940's as a means of solving problems in quantum-electrodynamics, but subsequently found extensive application in all areas employing the quantum-mechanical perturbation theory. In the diagram approach, the probability amplitude for our process is obtained by multiplying the amplitudes for subprocesses into which a given process can be divided. Mixing between the original states by the perturbing interaction is taken into account by introducing the probability amplitudes for transitions between the states. These amplitudes are given, as usual in quantum mechanics, by the matrix elements of the perturbing interaction that correspond to these transitions. The order of the perturbation-theory approximation is determined in the diagram technique by the number of transitions taken into account in the analysis of the process.

Questions relating to neutron helicity are most conveniently examined in a coordinate frame in which the quantization axis lies along neutron momentum. To simplify our analysis, we shall use angular momentum eigenfunctions with phases chosen as in Ref. 28.

In our case, the initial picture (zero-order perturbation theory) corresponds to the presence of one s-resonance and one p-resonance in the nucleus. It is described by the usual Breit-Wigner amplitudes for these resonances. The average amplitudes for unpolarized nuclei are given by the well-known expressions[29]

$$f_l^0(E)=-\frac{g}{2k}\,\frac{\Gamma_l^n(E)}{E-E_l+i\,(\Gamma_l/2)}, \qquad (12)$$
$$g=\frac{2J+1}{2\,(2I+1)},\quad \Gamma_l^n(E)=\Gamma_l^n(E_l)\left(\frac{E}{E_l}\right)^{l+(1/2)},$$

where k is the neutron wave number, E_l is the energy of the resonance, $\Gamma_l\Gamma_l^n$ are its total and neutron widths, and I and J are the spins of the original nucleus and of the resonance, respectively. The index l indicates the orbital angular momentum corresponding to the resonance. The p-resonance spin $J=I\pm(1/2)$ can be made up in different ways from the three angular momenta I, S, l participating in the process. In our case, it is convenient to use the following representation of the total angular momentum of the neutron:

$$\mathbf{j}=\mathbf{l}+\mathbf{s},\qquad j=\frac{1}{2},\ \frac{3}{2}. \qquad (13)$$

A given resonance can be excited by neutrons with either value of j or, in other words, along two possible channels. According to this the total neutron width Γ_p^n is the sum of channel widths Γ_{pj}^n:

$$\Gamma_p^n=\Gamma_{p1/2}^n+\Gamma_{p3/2}^n. \qquad (14)$$

For the s-resonance, the total angular momentum of the neutron is equal to its spin, and the process proceeds along a single channel:

$$\Gamma_s^n=\Gamma_{s1/2}^n. \qquad (15)$$

Parity-conserving elastic scattering of neutrons via a resonance can be represented by the simplest diagram shown in Fig. 1. This describes the capture of a neutron n by a nucleus A, followed by the formation of the compound nucleus $(A+1)_l^*$ (l indicates both the compound nucleus state and the orbital angular momentum of the neutron), and the subsequent decay of the compound nucleus to the original neutron and nucleus. The procedure used to obtain (12) for the amplitude for this process can be explained in a general way as follows. Suppose that, in the initial state, neutrons with a given momentum travel along the z axis and are polarized parallel to the momentum. They are described by a wave function of the form

$$\Psi=e^{ikz}\chi_{\pm}, \qquad (16)$$

where k is the neutron wave number. Consider processes due to neutrons with fixed values of l, j, j_z. The weight of the wave function in the original wave (16) for such neutrons can be readily obtained by considering the corresponding expansion. Apart from an unimportant factor, this weight is $\sqrt{2l+1}\,C_{\text{los}\,s_z}^{lj_z}$, where $C_{\text{los}\,s_z}^{lj_z}$ is the vector addition coefficient. The weight may be looked upon as the amplitude for the transition from the state (16) to the state $|l,j,j_z\rangle$ in which we are interested. The amplitude corresponds to the ingoing line n in the diagram. The amplitude for the formation of a state $|J,J_z\rangle$ of the resultant system by a neutron in the state $|j,j_z\rangle$ and a nucleus in the state $|I,I_z\rangle$ is $C_{lj_zII_z}^{JJ_z}$. The amplitude for the formation of the compound state $(A+1)_l^*$ from a

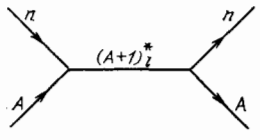

FIG. 1. Diagram representing the zero-order approximation.

nucleus A and a neutron with total angular momentum j is proportional to $\sqrt{\Gamma^{n}_{pj}}$, where the sign of this amplitude is characteristic for the state and is usually unknown. The product of the last two amplitudes may be regarded as associated with the ingoing vertex in the diagram. The resonance energy dependence, which is physically associated with the capture amplitude and is determined by the so-called propagator $\left(E-E_l+i\frac{\Gamma_l}{2}\right)^{-1}$, is conveniently assigned to the part of the diagram between the vertices. The outgoing part of the diagram (the outgoing vertex and outgoing lines) differs from the ingoing part merely by the fact that the process has been reversed. With our choice of the angular momentum eigenfunctions, the two are described by the same amplitudes except that decay into the elastic channel can proceed with any possible angular momentum j'. Multiplying the above amplitudes together, we obtain (apart from a constant factor A_0) the amplitude A for elastic forward scattering of neutrons from a plane wave with given s_z by a nucleus with given I_z. This only takes into account processes proceeding through a resonance with given l (s- or p-resonance) along the entrance channel with total neutron angular momentum j and along the exit channel with angular momentum j'. The expression for the amplitude is

$$A=A_0\sqrt{2l+1}C^{jj_z}_{l0s\,s_z}C^{JJ_z}_{jj_zII_z}\sqrt{\Gamma^{n}_{lj}}\frac{1}{E-E_l+i(\Gamma_l/2)}$$
$$\times C^{JJ_z}_{j'j'_zII_z}C^{j'j'_z}_{l0s\,s_z}\sqrt{\Gamma^{n}_{lj'}}\sqrt{2l+1}. \qquad (17)$$

If we sum (17) over j, j' and average over I_z, we obtain the average amplitude for unpolarized nuclei:

$$A^0_l(E)=A_0 g\frac{\sum_j \Gamma^{n}_{lj}}{E-E_l+i(\Gamma_l/2)}, \qquad (18)$$

which becomes identical with $f^0_l(E)$ when $A_0=-1/2k$. The magnitude of the constant A_0 depends on the normalization of the original plane wave (16) and the factors omitted from the expressions for the amplitudes for the subprocesses. The average amplitude that we have obtained does not depend on s_z or the signs of $\sqrt{\Gamma^{n}_{lj}}$. The fact that $A^0_l(E)$ is independent of s_z (neutron helicity) is not unexpected because this amplitude was deduced on the assumption of parity conservation.

The dependence on neutron helicity gives rise to corrections to the main amplitudes $A^0_l(E)$ obtained in first-order perturbation theory in the P-odd interaction W. This approximation takes into account the contribution to the amplitude of the two processes shown in Fig. 2. The first of them differs from that of Fig. 1 merely by the fact that its central portion now contains the transition from the compound state $(A+1)^*_l$ to the compound state $(A+1)^*_{l'}$,

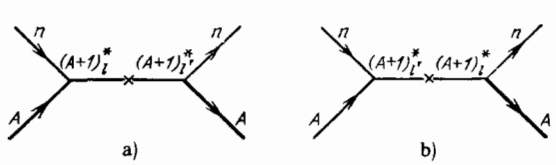

FIG. 2. Diagrams representing the first-order approximation.

which is produced by the interaction W and is indicated by the cross. The amplitude for this transition is considered to be given by the corresponding matrix element $W_{l'l}$. Its energy dependence, i.e., the propagator $\left(E-E_{l'}+i\frac{\Gamma_{l'}}{2}\right)^{-1}$, is usually assigned to the portion of the diagram between the transition and the outgoing vertex. The expression for the amplitude for the process in Fig. 2a is thus obtained from the amplitude (17) by replacing the propagator $\left(E-E_l+i\frac{\Gamma_l}{2}\right)^{-1}$ with the product $\left(E-E_l+i\frac{\Gamma_l}{2}\right)^{-1}\times W_{l'l}\left(E-E_{l'}+i\frac{\Gamma_{l'}}{2}\right)^{-1}$. In addition, the subscript l must be replaced with l' in factors after this product. Summation of the expression obtained in this way over j, j' followed by averaging over I_z gives the following expression in the case of an unpolarized target for the average additional amplitudes for neutrons with different helicities ($s_z=\pm 1/2$):

$$[f'_{ll'}(E)]_{\pm}=\mp\frac{g}{2k}\frac{\sqrt{\Gamma^{n}_{lj}}W_{l'l}\sqrt{\Gamma^{n}_{l'j}}}{[E-E_l+i(\Gamma_l/2)][E-E_{l'}+i(\Gamma_{l'}/2)]}, \qquad (19)$$

where j represents $j=1/2$, i.e., the possible common value for the two compound states under consideration. Expression (19) gives the absolute magnitude of the amplitude and shows that the amplitude changes sign when the neutron helicity is reversed. The absolute signs of the amplitudes obtained in this way are undetermined because (19) contains the factor $\sqrt{\Gamma^{n}_{lj}}\sqrt{\Gamma^{n}_{l'j}}$. The amplitude for the diagram of Fig. 2b differs from that given by (19) only by the reverse order of the factors and the replacement of $W_{l'l}$ with $W_{ll'}$. For our choice of the phases of the eigenfunctions we have $W_{l'l}=W_{ll'}$, and the total amplitude is obtained simply by multiplying the amplitude (19) by two. Thus, in first-order perturbation theory in the P-odd interaction W, we obtain the following expression for the helicity-dependent part of the forward-scattering neutron amplitude in the case of unpolarized target nuclei:

$$f'_{\pm}(E)=\mp\frac{g}{k}\frac{\sqrt{\Gamma^{n}_{s}(E)}W_{sp}\sqrt{\Gamma^{n}_{p1/2}(E)}}{[E-E_s+i(\Gamma_s/2)][E-E_p+i(\Gamma_p/2)]}. \qquad (20)$$

This is analogous to the expression obtained in Ref. 25, and we use the generally accepted notation for the parameters of the s- and p-resonances and the fact that $\Gamma^{n}_{s1/2}=\Gamma^{n}_{s}$.

P-odd effects in the elastic channel of the neutron-nucleus interaction (neutron-optical dichroism and birefringence) are conveniently characterized by the changes $\Delta\sigma$ and Δn in the total neutron cross section and refractive index for neutrons due to the reversal of neutron helicity, respectively. These are readily obtained with the aid of (7), (8), and (20)

$$\Delta\sigma=\sigma_+-\sigma_-=B[(E-E_s)\Gamma_p+(E-E_p)\Gamma_s],$$
$$\Delta n=n_+-n_-=-\frac{N}{k}B\left[(E-E_s)(E-E_p)-\frac{\Gamma_s\Gamma_p}{n}\right], \qquad (21)$$

where

$$B=\frac{2\pi}{k^2}\frac{gW_{sp}\sqrt{\Gamma^{n}_{s}(E)\Gamma^{n}_{p1/2}(E)}}{[(E-E_s)^2+(\Gamma^2_s/4)][(E-E_p)^2+(\Gamma^2_p/4)]}.$$

Expressions of the form given by (21) were first reported in Ref. 21, where they were obtained by using the R-matrix theory and the Born approximation.

Experimental studies of P-odd effects in the elastic channel have been carried out with neutron energy much closer to the p- than to the s-resonances. It will be clear from the ensuing discussion that this was so because the observed effects were much greater near the s-resonances. The expressions given by (21) become much simpler near the p-resonance:

$$\Delta\sigma \approx 2\mathscr{P}(E)\,\sigma_{\rm p}(E), \tag{22}$$

where

$$\mathscr{P}(E)=\frac{2W_{\rm sp}}{E-E_{\rm s}}\sqrt{\frac{\Gamma_{\rm s}^{\rm n}(E)}{\Gamma_{\rm p}^{\rm n}(E)}\frac{\Gamma_{\rm p1/2}^{\rm n}(E)}{\Gamma_{\rm p}^{\rm n}(E)}}$$

and $\sigma_{\rm p}(E)$ becomes the usual Breit-Wigner cross section for the p-resonance:

$$\sigma_{\rm p}(E)=\frac{\pi}{k^2}\frac{g\Gamma_{\rm p}^{\rm n}(E)\,\Gamma_{\rm p}}{(E-E_{\rm p})^2+(\Gamma_{\rm p}^2/4)}.$$

These expressions were obtained in Ref. 12, where P-odd effects in the elastic channel of the neutron-nucleus interaction were first examined in the compound-state mixing model. When theoretical calculations are compared with experimental data, it is convenient to express the change Δn in the refractive index in terms of $\Delta\sigma$. This expression has the form

$$\Delta n=-\frac{N}{k}\frac{E-E_{\rm p}}{\Gamma_{\rm p}}\Delta\sigma. \tag{23}$$

The energy denominator in the expression for $\mathscr{P}(E)$ appears because of dynamic enhancement of level mixing due to the fact that the levels have similar energies. The expression for $\mathscr{P}(E)$ contains one further factor that enhances the P-odd effects that we are considering near the p-resonances of complex nuclei. This is the kinematic factor

$$\sqrt{\frac{\Gamma_{\rm s}^{\rm n}(E)}{\Gamma_{\rm p}^{\rm n}(E)}\frac{\Gamma_{\rm p1/2}^{\rm n}(E)}{\Gamma_{\rm p}^{\rm n}(E)}},$$

which is usually large because $\Gamma_{\rm s}^{\rm n}\gg\Gamma_{\rm p}^{\rm n}$, and $\Gamma_{\rm p^{1/2}}^{\rm n}$ is probably of the same order as $\Gamma_{\rm p}^{\rm n}$. Expressions analogous to (22) and (23) can also be readily obtained when the neutron energy is close to an s-resonance. Here again, we have dynamic enhancement of level mixing, but kinematic enhancement is transformed into kinematic attentuation and produces a very considerable reduction in the size of the observable effects.

We note in connection with (23) that, although the absolute signs of the effects under consideration are, as noted above, undetermined, their relative sign is known if we know which p-resonance is responsible for the observed effects. This sign is given by the sign of the difference $E-E_{\rm p}$.

Finally, let us consider the range of validity of the above two-level approximation. The contributions to the above effects that are due to the mixing of a given p-resonance with any s-resonance of the same spin are described by expressions analogous to (22) and (23). The size of these effects is proportional to $\mathscr{P}(E)$. If we suppose that all the $W_{\rm sp}$ are equal to within an order of magnitude, and the s-resonances have comparable strength, the presence of the energy denominator $E-E_{\rm s}$ in $\mathscr{P}(E)$ will ensure that the main contribution to the effect will be provided by the nearest s-resonance. The two-level approximation may turn out to be inadequate when these conditions are not satisfied. This will most likely occur in nuclei with high density of resonances, in which the number of "nearest neighbors" is high.

3. EXPERIMENTAL STUDIES OF p-ODD EFFECTS IN THE ELASTIC CHANNEL OF THE NEUTRON-NUCLEUS INTERACTION

A. General remarks

Studies of the P-odd neutron-optical dichroism rely on measurements of the transparency of an unpolarized target as a function of neutron helicity. Usually measurements are made of the so-called transmission effect

$$\varepsilon=\frac{T_+-T_-}{T_++T_-}, \tag{24}$$

where $T_\pm=e^{-n\sigma_\pm}$ is the transparency of the target for neutrons with positive and negative helicity, respectively, and n is the target thickness expressed as the number of nuclei per square centimeter. When $n\Delta\sigma$ is small, and this is always the case in such measurements, the expression given by (24) becomes very much simpler:

$$\varepsilon=-n\frac{\Delta\sigma}{2}. \tag{25}$$

When the measurements are performed near a p-resonance, and the observed resonance is not appreciably broadened by the Doppler effect and inadequate energy resolution, the effective value of $\Delta\sigma$ is given by (22), and

$$\varepsilon(E)=-n\mathscr{P}(E)\,\sigma_{\rm p}(E). \tag{26}$$

Since $\mathscr{P}(E)$ is a slowly-varying function of energy, the function $\varepsilon(E)$ has a clear resonance in the neighborhood of the p-resonance, which is due to the energy dependence $\sigma_{\rm p}(E)$. Measurements of the P-odd dichroism in the immediate neighborhood of the p-resonance are best represented by $\mathscr{P}(E_{\rm p})$, since $\mathscr{P}(E)$ is practically constant and equal to $\mathscr{P}(E_{\rm p})$ within the limits of the resonance.

For very low energy neutrons (thermal and cold), $\Delta\sigma$ and ε cease to be functions of energy when measurements are performed in the immediate neighborhood of the p-resonance. This is so because the reduction in $\sigma_{\rm p}(E)$ with decreasing energy is compensated by the corresponding increase in $\mathscr{P}(E)$. For thermal and cold neutrons, it seems to us that the experimental results are best represented by the experimental value of $\Delta\sigma$.

When the P-odd neutron-optical birefringence is investigated, the neutron beam polarized at right angles to the momentum is transmitted by an unpolarized target and the rotation of the neutron polarization around the momentum, due to the neutron-nucleus interaction, is measured directly. Such measurements are methodologically more difficult than measurements of effects in total cross sections because they require a polarized beam and measurement of the rotation of its polarization. The experimental data are then best represented by the rotation $\Delta\varphi$ of polarization per unit target thickness. This is very simply related to the change Δn in the refractive index due to reversal of neutron helicity:

$$\Delta\varphi = -k\,\Delta n. \tag{27}$$

The relation between $\Delta\varphi$ and the parameters of the mixing resonances and matrix element of the P-odd interaction (when the neutron energy is relatively close to the p-resonance) can be readily deduced from (22) and (23). We again express the rotation of polarization in terms of the change in total cross section:

$$\Delta\varphi = N\,\frac{E-E_p}{\Gamma_p}\,\Delta\sigma. \tag{28}$$

The energy dependence of $\Delta\varphi$ is very different from that of ε. When $E = E_p$, we have $\Delta\varphi = 0$ and $\Delta\varphi$ has different signs for E on either side of E_p. $|\Delta\varphi|$ is a maximum for $|E - E_p| = \Gamma_p/2$, but then falls off, and this falling off is much slower than in $\varepsilon(E)$.

Since the P-odd effects are small, particular attention must be paid to the elimination of spurious effects, both systematic and random, when the effects are examined experimentally. Statistical uncertainties provide the main limitation on precision in the case of effects in the elastic neutron-nucleus interaction channel. It is therefore useful to consider the optimization of target parameters. The count rate can be increased by ensuring that the entire beam area is covered by the target. The effects that we are considering increase linearly with increasing target thickness, but the transmitted beam intensity decreases with target thickness, and there is a corresponding loss of statistical precision. Simple calculation shows that the optimum target attenuates the beam intensity by a factor of e^2.

In the three to four years since the first reports of experimental confirmations of P-odd effects in the elastic neutron-nucleus interaction channel, there have been relatively few papers on this topic. We continue with a brief review of the most important of these experiments.

B. Experiments with cold and thermal neutrons

We begin with the experiments[11] performed at the ILL in Grenoble, which were the first to succeed in detecting the effect that we are considering. These experiments were largely concerned with the rotation of neutron polarization around the neutron momentum in an unpolarized ^{117}Sn specimen. The results obtained on the total cross section of ^{117}Sn as a function of neutron helicity were of low precision and only preliminary. The experiments were performed with one of the beams from the high-flux ILL reactor. The beam area was about 1×1 cm, the flux was about 10^7 neutrons/cm^{2}s, and the neutron energy was about 1.7 meV.

The apparatus is illustrated schematically in Fig. 3. Two identical polarization-sensitive elements 1 and 8 were employed in the system. They were in the form of stacks of vertical and vertically magnetized Fe-Co mirrors which had a much higher reflectance for spin-up than for spin-down neutrons. Reflection by mirrors 1 was used to produce a beam with spin-up polarization $f_n \approx 0.9$. This beam was introduced into the region of low magnetic field by passing it nonadiabatically (without affecting the direction of polarization) through the special coil 2. The specimen under investigation (its possible positions are shown by the broken line in Fig. 3) and the auxiliary coils 3, 4 were placed in the low-field region which was protected from stray fields by the three-layer magnetic screen 5. The system used to determine the rotation of the neutron polarization around the direction of the beam consisted of the coil 6, the stack of mirrors 8, and the Li-glass neutron scintillation counter 9. The coil 6 was similar to coil 2, but was rotated through 90° relative to the latter. This ensured the nonadiabatic passage of neutrons from the low-field region to the region of the horizontal guiding field perpendicular to the beam. The polarization component perpendicular to the initial polarization, produced by the rotation under consideration, was thus made parallel to the field in the guiding-field region. Between coil 6 and mirrors 8, the guiding field gradually rotates until it becomes vertical, thus ensuring the corresponding adiabatic rotation of this polarization component. The polarization component under investigation is reversed by reversing the current in coil 6, which is accompanied by a corresponding change in the reflectance of mirrors 8. The rotation of the neutron polarization was determined by measuring the difference between counting rates in detector 9 when the neutrons were reflected by mirrors 8 for different directions of the current in coil 6. Effects due to the instability of the beam and instrumental parameters were minimized by frequently repeating the measurements for different directions of the current in coil 6 (at intervals of approximately 1″).

This system is not free from appreciable instrumental effects, especially when small rotations of polarization are measured. In fact, spurious effects are produced by the presence in the low-field region of the longitudinal field component and the fact that coils 2 and 6 are not strictly perpendicular. These effects are eliminated by the use of the auxiliary coil 4 and by performing the measurements with the specimens located before the coil 4 and after it. The field in coil 4 was vertical and produced a 180° precession of the neutron spins. This coil reversed the horizontal component of neutron polarization present at entry to the coil, but had no effect on the direction of the neutron polarization in the region behind the coil. The sign of the effect produced in the specimen could therfore be reversed by displacing the speci-

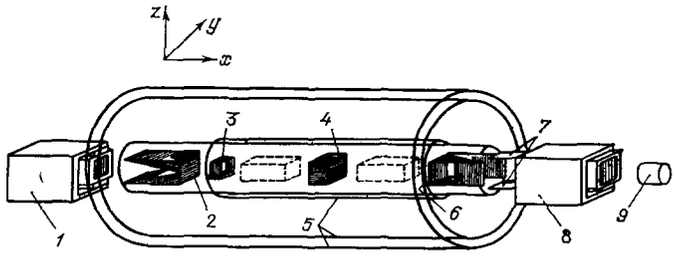

FIG. 3. Schematic illustration of the apparatus at ILL: 1, 8—stacks of Fe-Co mirrors; 2, 6—nonadiabatic transit coils; 3, 4—auxiliary coils; 5—magnetic screen; 7—shims; 9—detector.

men from one position to the other, and this was used to separate the required effect from instrumental factors.

Many control experiments and cross checks were necessary because the rotation of the direction of polarization was small. Judging by the published account,[11] it was considered that instrumental effects could be eliminated with a precision better than about 5×10^{-6} rad.

Measurements of the total cross section as a function of neutron helicity were much simpler. The longitudinal polarization necessary for these measurements was produced by using coil 3 (producing a longitudinal field) to rotate the direction of polarization into the horizontal position, and then rotating it again with coil 4 into the longitudinal position. The helicity of the beam was reversed by reversing the current in coil 4 (as in measurements of the angle of rotation, at intervals of about 1″). In these measurements, the specimen was always kept behind coil 4, whereas coil 6 and mirrors 8 were removed from the beam.

Measurements of the rotation of direction of polarization were performed for a specimen of natural Sn ($11\times11\times60$ mm^3) and an enriched specimen containing up to about 84% of ^{117}Sn ($11\times11\times49.5$ mm^3). The following results were obtained:

$$\Delta\varphi\ (\text{Sn nat.}) = (-4{,}9 \pm 0{,}9)\cdot10^{-6}\ \text{rad/cm},$$
$$\Delta\varphi\ (^{117}\text{Sn}) = (-36{,}7 \pm 2{,}7)\cdot10^{-6}\ \text{rad/cm},$$
$$\Delta\sigma\ (^{117}\text{Sn}) = (10{,}2 \pm 4{,}0)\cdot10^{-29}\ \text{cm}^2.$$

This value of $\Delta\sigma$ was obtained by calculation from the value of ε reported in Ref. 11. The sign of $\Delta\varphi$ has been reversed as compared with that in Ref. 11 in view of a recent report.[30] The latter also points out that the Grenoble system has been improved to ensure greater precision of measurement. The measurements of $\Delta\varphi$ have been repeated with the improved system, using natural tin and lead:

$$\Delta\varphi\ (\text{Sn nat.}) = (-3{,}2 \pm 0{,}4)\cdot10^{-6}\ \text{rad/cm},$$
$$\Delta\varphi\ (\text{Pb nat.}) = (2{,}2 \pm 0{,}3)\cdot10^{-6}\ \text{rad/cm}.$$

Comparison of rotations determined for natural and enriched tin shows that the experiment is correct because their ratio is in agreement, to within experimental error, with the corresponding concentration of ^{117}Sn in the natural mixture.

Let us now consider the experiments[13,14] performed at the Leningrad Institute for Nuclear Physics by the Lobashov group, using the VVR-M reactor at the Institute. A beam of polarized thermal neutrons ($E\simeq0.01$ eV) with beam area of about 6×1 cm^2 was employed. The neutron flux was about 10^7 cm^{-2}s^{-1} and the polarization was $f_n\approx0.9$.

A simplified diagram of the system is shown in Fig. 4. A transversely-polarized neutron beam was introduced through the neutron pipe 1 into the radio-frequency reversing system 2. Li collimators were used after this reversing system to separate the beam into two parallel components that were adiabatically introduced into the two solenoids 4 whose longitudinal fields had opposite directions, so that the beam neutrons had opposite helicities. Identical specimens 3 were placed in each of the beams in the solenoids. Neutrons transmitted by these specimens were recorded by ^{3}He proportional counters 6 with a common gas-filled volume. The difference between the count rates produced by these detectors as functions of the neutron helicity were used to determine the total cross sections as functions of helicity.

The use of the two-beam arrangement and the simultaneous measurement of the effects in two specimens placed in beams of opposite helicity produced a considerable reduction in the effect of beam instability on the final results. The beam helicity was reversed in the course of measurements at two-second intervals, using the reversal system. Pulses from each of the detectors were integrated at constant beam helicity. Charges from the two detectors acquired over the two-second interval, and the difference between them, were converted into a digital code which was sent on to a recording system. The beam helicities were then reversed and the sequence repeated. The field directions in the solenoids containing the specimens were reversed after each twelve hours of such measurements. This reversed the sign of the effect under consideration and was used to check for the absence of spurious effects.

Working measurements were accompanied by control measurements under the same conditions, but with unpolarized beams. The beams were depolarized by a thin iron shim placed in front of the reversing system. Measurements showed that there were no appreciable instrumental effects.

In addition to the effects in the total cross sections, a study of the n, γ-reaction was also carried out, using only one solenoid with a longitudinal field and one specimen. The γ-rays were recorded by two sodium iodide scintillation counters (crystals 150 mm in diameter and 100 mm thick), located on either side of the solenoid containing the specimen. These measurements show that practically the entire helicity dependence of the cross section was due to the n, γ-reaction, i.e., processes proceeding through the compound nucleus.

Specimens investigated included ^{117}Sn, ^{139}La, and natural Br (50% ^{79}Br and 50% ^{81}Br). The specimen thickness was equivalent to one or two neutron mean free paths. We have calculated the following values of $\Delta\sigma=\sigma_+-\sigma_-$ from these experimental results:

$$\Delta\sigma\ (^{117}\text{Sn}) = (4{,}6 \pm 0{,}5)\cdot10^{-29}\ \text{cm}^2,$$

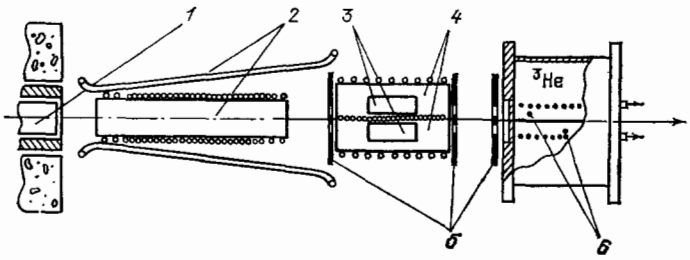

FIG. 4. Schematic illustration of the apparatus at the Leningrad Institute of Nuclear Physics: 1—neutron pipe; 2—reversing system; 3—specimens; 4—solenoids; 5—collimators; 6—detectors.

$$\Delta\sigma\ (^{139}\mathrm{La}) = (34{,}2 \pm 5{,}3)\cdot 10^{-29}\ \mathrm{cm}^2,$$
$$\Delta\sigma\ (\mathrm{Br}) = (60{,}6 \pm 6{,}2)\cdot 10^{-29}\ \mathrm{cm}^2.$$

The calculation for Br was carried out on the assumption that the effect was entirely due to one isotope.

C. Experiments with resonance neutrons

These experiments were performed at Dubna in the Neutron Physics Laboratory of the Joint Institute for Nuclear Research. Measurements were carried out of the energy dependence of the total cross section for different directions of neutron helicity. They were performed for a number of nuclei at energies near the low-energy p-resonances of these nuclei. The time-of-flight technique was used with a beam of polarized resonance neutrons from the IBR-30 pulsed reactor.[31] The neutrons were polarized by passing them through a polarized proton target.[19] This technique was developed at the Neutron Physics Laboratory at Dubna. An improved target was employed as compared with the experiments reported in Ref. 31. The useful target area (beam area) was increased by a factor of three and amounted to 30 cm^2. The length of the flight path was 58 m. In the case of resonances with energies up to about 1.5 eV, the reactor was operated so as to produce neutron bursts of about 70 μs with a mean power of about 20 kW. At higher energies, energy resolution was improved by using the booster regime in which the burst length was about 4 μs and the mean power about 5 kW.

The apparatus is illustrated schematically in Fig. 5. The unpolarized neutron beam from reactor 1 was passed through the evacuated neutron pipe 2 and eventually intercepted by the polarizer at a distance of 32 m from the reactor. The polarizer was in the form of a proton target 4 with lateral dimensions of 5×6 cm^2. It was located in a horizontal magnetic field perpendicular to the beam. The collimator 3 with dimensions somewhat smaller than that of the target was placed in front of the proton target. Filtration of the beam by the polarized proton target produced its polarization because the singlet neutron-scattering cross section of protons is much greater than the triplet cross section. The proton target ensured that the polarization of the resonance neutrons was $f_n \approx 0.6$ for an intensity loss by a factor of about 10. The transversely-polarized beam leaving the proton target was directed into the gap of the electromagnet 5 producing a field of about 200 Oe whose direction was the same as the field in the proton target. Magnet 5 was followed by a similar electromagnet 7 whose field could be made either parallel or antiparallel to that of magnet 5 by simply reversing the current in its coils. A thin foil 6 perpendicular to the beam was placed half-way between the magnets. The magnetic field in this foil due to magnet 5 had the same direction as the field in the magnet. When the fields in magnets 5 and 7 had opposite directions, the field in the foil produced the conditions for a nonadiabatic transmission of neutrons, so that the polarization of the beam leaving the foil was reversed relative to the direction of the field. Magnet 7 was followed by solenoid 10 producing a 200 Oe longitudinal field in the direction of the neutron momentum. The magnetic field rotated gradually from the transverse direction to the longitudinal direction along the path between magnet 7 and the solenoid, and this produced an adiabatic rotation of the direction of polarization of the beam. The adiabatic condition was adequately satisfied for neutrons with energies up to ≈ 100 eV. This arrangement produced a longitudinally polarized beam with helicity determined by the direction of the current in the coils of magnet 7. Specimens 9 were placed in the neutron beam formed by collimator 8. Neutrons transmitted by the specimen reached the neutron detector 12 along the evacuated neutron pipe 11. The detector was a γ-ray scintillation counter with an n, γ-converter, or a scintillation counter incorporating Li glass. The time spectra produced by the detector were recorded by an automatic system controlled by a small computer which was also used to control the reversal of the beam helicity.

In working measurements, the direction of the beam polarization was reversed at intervals of 40 s, and the two time spectra N_p and N_a corresponding to polarization respectively parallel and antiparallel to the neutron momentum were acquired. Measurements on each specimen were continued for 150–200 hours. The resultant $N_{p,a}$ spectra channel for each specimen were used to determine for each channel the magnitude of the transmission effect

$$\varepsilon = \frac{1}{f_n}\,\frac{N_p - N_a}{N_p + N_a} = \frac{T_+ - T_-}{T_+ + T_-}. \qquad (29)$$

The total cross section was investigated as a function of neutron helicity for 14 resonance nuclei: ^{81}Br ($E_0 = 0.9$ eV), ^{93}Nb ($E_0 = 36$ eV, 42 eV), ^{11}Cd ($E_0 = 4.5$ eV; 6.9 eV), ^{117}Sn ($E_0 = 1.3$ eV), ^{127}I ($E_0 = 7.6$ eV; 10.4 eV; 14.0 eV), ^{139}La ($E_0 = 0.75$ eV), ^{145}Nd ($E_0 = 2.0$ eV), ^{238}U ($E_0 = 4.4$ eV; 11.3 eV–19.5 eV).Except for the two known resonances in ^{93}Nb, all these are only tentatively identified as resonances because they are weaker by several orders of magnitude than the mean s-resonances of the corresponding nuclei. Three of these resonances (one each in Br, I, and Nd) were previously unknown and were discovered at Dubna in special measurements of the transmission of thick specimens. Since isotope-separated Br specimens were not available, the isotopic identification of the Br resonance was based on measurements of γ-ray spectra due to radiative neutron capture.

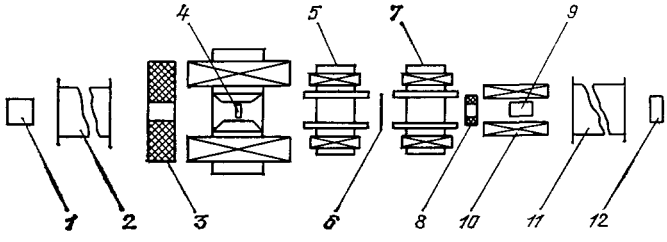

FIG. 5. Schematic diagram of the apparatus at the Neutron Physics Laboratory of the Joint Institute for Nuclear Research: 1—reactor; 2, 11—neutron pipe; 3, 8—collimators; 4—polarized proton target; 5, 7—electromagnets producing the guiding field; 6—thin foil; 9—specimen; 10—solenoid; 12—detector.

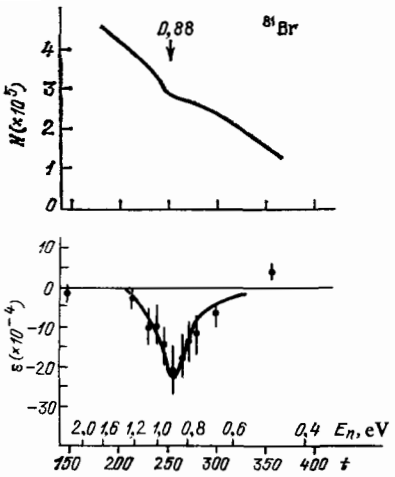

FIG. 6. Part of the time-of-flight spectrum and the transmission effect for Br.

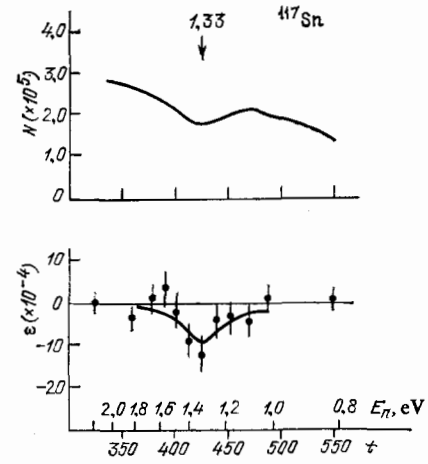

FIG. 8. Part of the time-of-flight spectrum and transmission effect for Sn.

Figures 6–9 (upper graphs) show portions of the N_p spectra acquired over about 50 hours in the region of the p-resonances under investigation, for which the dependence of the total cross section on neutron helicity was confirmed. In these figures, E_n is the neutron energy in eV and t is the time of flight in arbitrary units. The positions and energies of the p-resonances are shown by the arrows and numbers at the top. The lower graphs in Figs. 6–9 show values of ε for the corresponding specimens and energies. These values are averages over channel groups in which the number of channels per group increases as the effect decreases. The experimental points on these graphs are placed at the midpoint of the energy intervals over which averages were taken. When the resonances under investigation are not broadened by the Doppler, effect and inadequate energy resolution, the transmission effect is related to $\mathscr{P}(E)$ by (26). However, when the resonance is appreciably broadened, the relationship becomes more complicated.[18] Table I lists the values of $\mathscr{P}(E_p)$ calculated from the values of ε given in Figs. 6–9, using these relationships and the necessary data on the parameters of p-resonances and experimental conditions. The resonance-parameter values employed in these calculations are also listed in the table. These parameters were deduced from the time spectra acquired in the course of measurements of transmission as a function of neutron helicity.

In principle, the relations given by (22) can be used to calculate the matrix element W_{sp} from $\mathscr{P}(E_p)$. However, in practice, this calculation is not unambiguous because the spins of the p-resonances are unknown, i.e., it is not known which s-resonance mixes with the given p-resonance. Moreover, there is no information about the quantity $\sqrt{\Gamma^n_{p1/2}}$ in (22). Table I lists the values of $|W_{sp}|$ calculated from (22) on the assumption that $\Gamma^n_{p1/2} = \Gamma^n_p$ and that the given p-resonance mixes with an s-resonance with the maximum value of $\Gamma^n_s/(E_p - E_s)^2$. The parameters of these resonances, taken from Ref. 32, are also listed in Table I. These calculations yield the required estimate of $|W_{sp}|$ within the framework of the two-level model.

The transmission effect was not detected (to within experimental error) for the other ten resonances that were investigated. For these resonances, the resulting values of ε were averaged over each resonance and, after the necessary

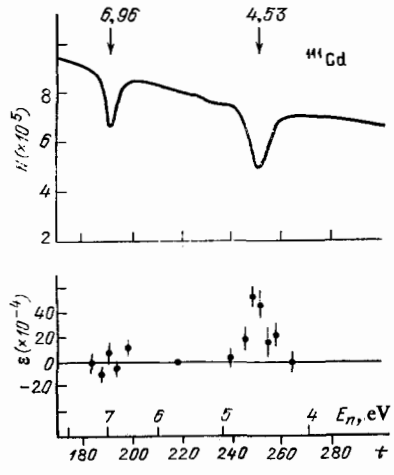

FIG. 7. Part of the time-of-flight spectrum and the transmission effect for Cd.

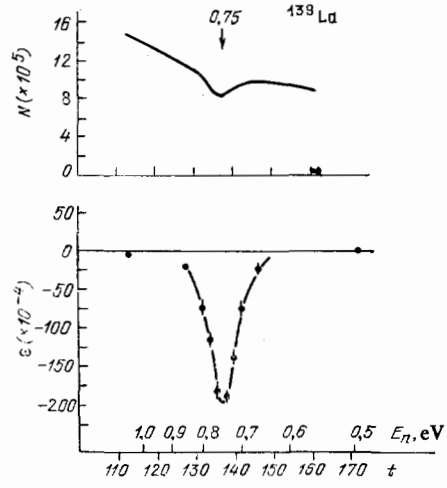

FIG. 9. Part of the time-of-flight spectrum and transmission effects for La.

TABLE I.

Nucleus	E_p, eV	Γ_p, 10^{-3}, eV	$g\Gamma_p^n$, 10^{-8} eV	E_s, eV	$g\Gamma_s^n$, 10^{-3} eV	$\mathscr{P}(E_p)$, 10^{-3}	$\lvert W_{sp}\rvert$, 10^{-3} eV
^{81}Br	0.88±0,01	190±20	5.8±0.3	101	10	24±4	3,0±0,5
^{111}Cd	4.53±0,03	160±10	107±5	−4	1,0	−8,6±1,2	0.84±0,12
^{117}Sn	1.33±0,01	230±20	19±1.5	−29	5.5	4.5±1,3	0.38±0,10
^{139}La	0.75±0,01	45±5	3.6±0.3	−49	84	73±5	1,28±0,12

processing, gave the upper limit for $\mathscr{P}(E_p)$. These estimates lie between 0.3×10^{-3} and 4×10^{-3}, and become increasingly crude as the energy of the resonance is increased or its strength is reduced, which is due to the rapid deterioration in the conditions of measurement.

4. DISCUSSION OF RESULTS

In the model in which the *P*-odd effects in complex nuclei are explained by the mixing of compound states of different parity, the values of the matrix elements W_{sp} are distributed around a zero mean. The measured values of $|W_{sp}|$ (see Table I) are in reasonable agreement with the estimated possible deviations of W_{sp} from zero, which were reported in Refs. 12 and 22. These values are distributed between 0.4×10^{-3} and 3×10^{-3} eV, and their lower bound is essentially determined by the experimental precision. Higher precision and greater range of resonances will be necessary for further verifications of the model. This should result in more reliable experimental distribution of W_{sp} and a corresponding comparision with theoretical predictions.

It is important to note, however, that the great paucity of data on the spins and parities of weak resonances gives rise to a considerable complication of the problem. It not only means that reliable values of $|W_{sp}|$ cannot be determined from the measured $\mathscr{P}(E_p)$, but also complicates measurements of ε. Attempts to detect the weak *P*-odd effect for a randomly chosen weak resonance are very laborious, and there is a high probability that the particular resonance will not turn out to be a p-resonance at all or, if it is a p-resonance, its spin is unsuitable for mixing with the s-resonances. The latter circumstance explains, at least partially, the absence of the effect in 10 and of the 14 weak resonances examined in Refs. 15–16. In this situation, it is very interesting to consider those cases for which it has been reliably established that the given resonance is a p-resonance and has spin $I \pm 1/2$. Unfortunately, here again, the situation is not simple. Such resonances are known only at energies of about 50 eV and above, where it is difficult to ensure sufficient experimental precision. Measurements of the *P*-odd effects in ^{93}Nb are an example of this. The following values of $\mathscr{P}(E_p)$ were obtained for the above two p-resonances:

$$\mathscr{P}(E_p = 36\ \text{eV}) = (2{,}0 \pm 1{,}3)\cdot10^{-3},$$

$$\mathscr{P}(E_p = 42\ \text{eV}) = (0{,}3 \pm 2{,}4)\cdot10^{-3}.$$

The experimental precision attained in these experiments was insufficient for the detection of effects that would be expected if the corresponding matrix elements were of the order of 10^{-3} eV.

Finally, we must consider the results of measurements of *P*-odd effects in the elastic channel of the neutron-nucleus interaction, obtained by using thermal and cold neutrons. With the exception of lead, the p-resonances responsible for the above effects are known for all the nuclei for which the effects were, in fact, observed, and the measurements of $\Delta\sigma$ were performed for these resonances. The *P*-odd rotation of neutron polarization in lead is difficult to explain in terms of the mixing of compound states. The lead isotopes have generally a low level density, and there are no weak resonances at low energies that could be interpreted as p-resonances responsible for the effects. Moreover, lead has no s-resonances suitable for mixing. Of course, it may be that the two levels associated with the effect lie below the neutron binding energy, but this is a relatively artificial assumption.

It is interesting to compare measurments on the p-resonances with the results for thermal neutrons. If we use (12) and (21), we can readily obtain the relationship connecting the thermal cross section $\Delta\sigma_{th}$ with $\mathscr{P}(E_p)$ and the p-resonance parameters. This expression is

$$\Delta\sigma_{th} \approx 2\sigma_p(E_p)\,\mathscr{P}(F_p)\left(\frac{\Gamma_p}{2E_p}\right)^2. \qquad (30)$$

Table II lists the values of $\Delta\sigma_{th}$ determined with thermal neutrons and the values of $\Delta\sigma_{th}^*$ calculated from (30),using measurements on the p-resonances. For ^{81}Br and ^{139}La, the agreement between $\Delta\sigma_{th}$ and $\Delta\sigma_{th}^*$ may be regarded as satisfactory. In the case of ^{117}Sn, $\Delta\sigma_{th}$ taken from Ref. 11, and obtained there with low precision, is also in agreement with $\Delta\sigma_{th}^*$, whereas $\Delta\sigma_{th}$ taken from Ref. 13 is too low.

Experimental data on *P*-odd rotation of the direction of neutron polarization can be compared with the dependence of the total cross section on helicity only for ^{117}Sn. This can be based on (28). If we use this relation to calculate the expected $\Delta\varphi^*$, using $\Delta\sigma_{th}$ and $\Delta\sigma_{th}^*$ taken from Table II, we obtain the results listed in Table III together with the value of $\Delta\varphi$ taken from Ref. 11. It is clear from Table III that $\Delta\varphi$ and $\Delta\varphi^*$ are in good agreement with one another although a somewhat higher value of $\Delta\sigma_{th}$ would be necessary to improve the degree of agreement,[13] just as in the case of Table II. The results of the latter comparisons show that the mixing of compound states provides a very good description of

TABLE II.

Nucleus	$\Delta\sigma_{th}$, 10^{-29} cm^2	$\Delta\sigma_{th}^*$, 10^{-29} cm^2
^{81}Br	60.6±6.2[14]	52±16
^{117}Sn	4.6±0.5[13]	9.8±4.1
	10.2±4.0[11]	
^{139}La	34.2±5.3[13]	35±11

TABLE III.

$\Delta\varphi$, 10^{-5} rad/cm (Ref. 11)	$\Delta\varphi^*$, 10^{-5} rad/cm (Ref. 11)	$\Delta\varphi^*$, 10^{-5} rad/cm (Ref. 13)	$\Delta\varphi^*$, 10^{-5} rad/cm (Ref. 15)
-3.7 ± 0.3	-2.3 ± 1.0	-1.1 ± 0.2	-2.5 ± 1.1

the energy dependence of $\Delta\sigma$, especially if we recall that the measured values of $\Delta\sigma$ obtained for the p-resonances differ from those for thermal neutrons by many orders of magnitude.

We note in conclusion that the *P*-odd effects in the elastic channel of the neutron-nucleus interaction are of considerable interest for nuclear physics. The study of these effects will lead to a better understanding of the complicated structure of the atomic nucleus and its excited states. As far as the possible determination from such data of specific information about the *P*-odd nucleon-nucleon interaction is concerned, the prospects for this are very limited. The effects that we have discussed are relatively readily observed only for intermediate and heavy nuclei for which the dynamic enhancement of the mixing of compound states is considerable. Under favorable conditions, such studies can be used to obtain the values of the corresponding matrix elements of the *P*-odd interaction. Unfortunately, the structure of the compound states of these nuclei is too complicated to offer us any prospect that the matrix elements could be used to deduce information about the details of the nucleon-nucleon interaction. We may expect, however, that, as more experimental data become available, some statistical information on this question will be obtained.

The author wishes to thank I. M. Frank for his interest in the preparation of this review and for useful suggestions, and L. B. Pikel'ner who provided the initial stimulus for the writing of this review and took part in fruitful discussions of many of the problems touched upon in this article.

[1]Yu. G. Abov *et al.*, Phys. Lett. **12**, 25 (1964).
[2]V. M. Lobashov *et al.*, Pis'ma Zh. Eksp. Teor. Fiz. **3**, 268 (1966) [JETP Lett. **3**, 173 (1966)].
[3]G. V. Danilyan *et al.*, ibid **26**, 197 (1977) [JETP Lett. **26**, 180 (1977)].
[4]Yu. G. Abov and P. A. Krupchitskiĭ, Usp. Fiz. Nauk **118**, 141 (1976) [Sov. Phys. Usp. **19**, 75 (1976)].
[5]F. C. Michel, Phys. Rev. B **329**, 133 (1964).
[6]L. Stodolsky, Phys. Lett. B **50**, 352 (1974).
[7]G. Karl and D. Tadic, Phys. Rev. C **16**, 172 (1977).
[8]M. Forte, Phys. Conf. Ser. No. 42, Ch. 5, 86 (1978).
[9]L. Barroso and D. Tadic, Nucl. Phys. A **294**, 376 (1978).
[10]V. A. Karmanov and G. A. Lobov,Pis'ma Zh. Eksp. Teor. Fiz. **10**, 332 (1969) [JETP Lett. **10**, 212 (1969)]; G. A. Lobov, Izv. Akad. Nauk SSSR Ser. Fiz. **34**, 1141 (1970).
[11]M. Forte *et al.*, Phys. Rev. Lett. **45**, 2088 (1980).
[12]O. P. Sushkov and V. V. Flambaum, Pis'ma Zh. Eksp. Teor. Fiz. **32**, 377 (1980) [JETP Lett. **32**, 352 (1980)].
[13]E. A. Kolomensky *et al.*, Phys. Lett. B **107**, 272 (1981).
[14]E. A. Vesna *et al.*, Pis'ma Zh. Eksp. Teor. Fiz. **35**, 351 (1982) [JETP Lett. **35**, 433 (1982)].
[15]V. P. Alfimenkov *et al.*, Pis'ma Zh. Eksp. Teor. Fiz. **34**, 308 (1981) [JETP Lett. **34**, 295 (1981)].
[16]V. P. Alfimenkov *et al.*, *ibid.* **35**, 421 (1982) [**35**, 51 (1982)].
[17]V. P. Alfimenkov *et al.*, Preprint No. R3-82-86. OIYaI, Dubna, 1982.
[18]V. P. Alfimenkov *et al.*, Nucl. Phys. A **398**, 93 (1983).
[19]Yu. V. Taran and F. L. Shapiro, Zh. Eksp. Teor.Fiz. **44**, 2185 (1963) [Sov. Phys. JETP **17**, 1467 (1963)].
[20]L. Stodolsky, Phys. Lett. B **96**, 127 (1980).
[21]V. E. Bunakov and V. P.Gudkov, Z. Phys. **303**, 285 (1981).
[22]O. P. Sushkov and V. V. Flambaum, Usp. Fiz. Nauk **136**, 3 (1982) [Sov. Phys. Usp. **25**, 1 (1982)].
[23]G. A. Lobov, Preprint No. 20, ITEF, Moscow, 1982.
[24]I. S. Shapiro, Pis'ma Zh. Eksp. Teor. Fiz. **35**, 275 (1982) [JETP Lett. **35**, 344 (1982)].
[25]O. P. Sushkov and V. V. Flambaum, Preprint No. 83-24, IYaF SO AN SSSR, Novosibirsk, 1983.
[26]S. G. Kadmenskiĭ *et al.*, Yad. Fiz. **37**, 581 (1983) [Sov. J. Nucl. Fiz. **37**, 345 (1983)].
[27]D. F. Zaretskiĭ and V. K. Sirotkin, *ibid.* **37**, 607 (1983) [**37**, 361 (1983)].
[28]A. M. Baldin *et al.*, Kinematika yadernykh reaktsiĭ (Kinematics of Nuclear Reactions), Fizmatgiz, Moscow, 1959.
[29]L. D. Landau and E. M. Lifshitz, Kvantovaya mekhanika, Fizmatgiz, M., 1963. [Engl. Transl. Quantum Mechanics, Pergamon Press, Oxford, 2nd ed. 1965, 3rd ed. 1977].
[30]B. R. Heckel, Private Communication, 1982.
[31]I. M. Frank, Fiz. Elem. Chastits At. Yadra **2**, 807 (1972) [*sic*].
[32]S. F. Mughabghab *et al.*, in: Neutron Cross Sections, Academic Press, New York, 1981, Vol. 1, Part. A.

Translated by S. Chomet